UDC 625.8
DOI: 10.15587/1729-4061.2025.327147

IDENTIFYING THE STRESS-STRAIN STATE OF RAILROAD OVERPASS SPANS

Ivan Bondar
Candidate of Technical Sciences (PhD), Associate Professor
Department of Aerospace and Transport Engineering
ALT University
Shevchenko str., 97, Almaty, Republic of Kazakhstan, 050013
Seidulla Abdullayev
Corresponding author
Doctor of Technical Sciences, Professor*
E-mail: s.abdullayev@satbayev.university
Arailym Tursynbayeva
Master Degree, Senior Lecturer*
Asel Abdullayeva
Master Degree, Senior Lecturer
Institute of Automation and Information Technologies**
Yerlan Auyesbayev
Doctor of Technical Sciences, Associate Professor
Academy of Architecture, Construction and Design
Caspian University
Seifullin ave., 521, Almaty, Republic of Kazakhstan, 050000
Aliya Izbairova
Candidate of Technical Science, Associate Professor*
*School of Transport Engineering and Logistics named after M. Tynyshpayev**
**Satbayev University
Satbayev str., 22, Almaty, Republic of Kazakhstan, 050000

This paper presents the results of the study of stress-strain state of reinforced concrete spans of two overpasses. With increasing volumes of cargo transportation by rail, the axle load increases up to 25 tons. Bridges and overpasses built about 100 years ago have acquired hidden defects during the years of operation. The safe operation of artificial structures requires additional research using the TENZO software and hardware complex, which processes digital records from primary transducers based on strain gauges. In 2018 and 2023, deflections, strains and stresses were obtained for typical beam spans of 11.5 m and 16.5 m of two reinforced concrete overpasses, from static and dynamic loads. For example, in 2018, the "spread" of stresses from the test load (TEM18) for the right-hand blocks of the 11.5 m spans ranged from 3.7 MPa to 3.71 MPa at different loading stages, and for the left-hand blocks of the 11.5 m spans ranged from 3.46 MPa to 3.9 MPa at different loading stages. In 2023, the stress range was from 2.58 MPa to 4.65 MPa for the right span blocks of 11.5 m span and from 2.67 MPa to 4.7 MPa for the left span blocks at different stages of loading. The 2018 data show uneven loading of the span blocks, indicating that the track axis is offset from the axis of the transportation structure. In 2023, the span structure blocks worked uniformly, which indicates that the track axis and the axis of the transportation structure are aligned (coincide). The obtained dependences "deformations and stresses" for typical beam spans of 11.5 m show the technical condition of the structures of the investigated objects, confirming the possibility of increasing the passage through them of a larger tonnage of transported cargo (increase in axial load up to 25 tons per axle). The spans have demonstrated reliable behavior under dynamic loads, with no signs of significant degradation in the period from 2018 to 2023. The use of data from scientific monitoring methods with the use of digital hardware and software systems will significantly reduce the cost of maintaining artificial structures on railroads and improve the safety of transportation infrastructure

Keywords: railroad overpass, span structure, monitoring system, stress-strain state, deformations, strains, stresses

Received 31.03.2025
Received in revised form 26.05.2025
Accepted 12.06.2025
Published 27.06.2025

How to Cite: *Bondar, I., Abdullayev, S., Tursynbayeva, A., Abdullayeva, A., Auyesbayev, Y., Izbairova, A. (2025). Identifying the stress-strain state of railroad overpass spans. Eastern-European Journal of Enterprise Technologies, 3 (7 (135)), 14–28. https://doi.org/10.15587/1729-4061.2025.327147*

1. Introduction

The issues of interaction of rolling load with the railway track and transportation facilities are relevant worldwide, as the increase in axle load leads to significant deformations and rapid wear of all elements, which adversely affects the operation of transport infrastructure and safety of people. In the Republic of Kazakhstan, the norms of designing and construction of artificial constructions are being revised taking into account foreign experience of more developed countries (Germany, Poland, Japan, USA, etc.). Kazakhstan mainline develops monitoring network systems for tracking and prediction (detection) of defects in the upper structure of the railroad track (rails, fasteners, sleepers), artificial structures (metal and reinforced concrete bridges, overpasses, pipes) based on the principles of strain gauges and dynamics (vibration sensors – accelerometers and visilometers).

Monitoring – continuous control over the technical condition of artificial structures at the operational stage plays a critical role in ensuring the sustainability and safety of railway infrastructure. The importance of this research lies in the growing need for maintaining the integrity and operational reliability of artificial structures, particularly on the railway network of the Republic of Kazakhstan, which operates under extreme natural and climatic conditions. In a rapidly evolving technological landscape, maintaining these structures efficiently is becoming more complex, requiring the adoption of advanced methods and technologies. The integration of continuous monitoring systems can significantly reduce the operational costs related to the maintenance of

artificial structures, optimize repair schedules, and enhance the safety of the infrastructure.

As the railway infrastructure ages and operational loads increase, it is crucial to plan maintenance strategies based on reliable, real-time data about the physical condition of the artificial structures. This data-driven approach facilitates more accurate predictions regarding the timing of repairs and the development of more effective preventive measures, thus extending the service life of these structures and minimizing unexpected failures. Consequently, the automation of design solutions for repairs and preventive measures, aligned with the real-time technical condition of artificial structures, has become a relevant challenge. This need for precision and timeliness is exacerbated by the continued expansion of Kazakhstan's railway network, where artificial structures play a pivotal role in ensuring safe and efficient transportation.

Stresses and dynamic coefficients are determined by both calculation and experimental methods for beam spans of bridges subjected to static and dynamic impacts from rolling stock. Moreover, the calculated stresses from the impact of dynamic load are added to the calculated stresses from the impact of static load. Designers, as a rule, recheck the data obtained by the calculation method, comparing them with the data obtained experimentally during testing of existing typical bridge spans. For beam spans of operational bridges, there is a database of dynamic coefficients, deformations, stresses, and displacements accumulated over a long period of monitoring the condition of supporting structures. The studies on the experimental determination of the stress-strain state of bridge span structures of railway bridges, presented in the works specialists, confirm the adequacy of the results presented in this article.

Therefore, research dedicated to the development of effective monitoring methods for artificial structures, with a focus on stress-strain analysis and real-time data utilization, is highly relevant. Such studies are necessary not only to improve the reliability of existing infrastructure, but also to develop future design standards and maintenance protocols that will ensure the long-term safety and functionality of railroad infrastructure.

2. Literature review and problem statement

The paper [1] presents the results of the study of interaction of rolling stock with frame structures of transportation facilities. It is shown that the results obtained by strain gauge method have practical significance. But the issues related to the sticking of strain gauges on the structures of span structures. The reason for this may be objective difficulties associated with the permission to open the protective layer of concrete, so fiber stresses were taken as initial data.

In [2], it is shown that the natural modes of operation of railroad trestles under the influence of rolling stock. However, there are issues that do not cover prestressed flyover structures. This is related to the prohibition to open the protective layer of concrete, as the operational services do not allow for coring in such structures at railroad facilities.

The paper [3] presents the results of investigation by finite element modeling of locomotive wheel. But the issues related to the study of the stress-strain state of the locomotive wheel flange are very ambiguous. The reason for this may be (objective difficulties associated with the comparison of full-scale studies and comparison with practical data obtained during the experiment.

In [4], the issues of permissible speed of locomotives on the railroad tracks of the Republic of Kazakhstan are considered. However, the issues related to speed limits on main lines remain open. The reason for this may be objective difficulties associated with the peculiarities of the rheology of soil embankments, salinity of most of the land through which the railroad tracks pass, as well as not perfect track structure, which makes the relevant study inappropriate for these sites.

In work [5], the locomotive fleet of the Republic of Kazakhstan is presented, but the issues related to the renewal of rolling stock for the last 5 years are not considered in this work. The emergence of shunting transport operating at stations and junctions reveals certain difficulties in the operation of such rolling stock. It is necessary to continue research in this direction.

The paper [6] describes the prospects of using gondola cars on bogies of ZK1 model in the organization of heavy freight transportation in the Republic of Kazakhstan. But the issues related to the impact of wheels on rails on curves and switches are not sufficiently studied. The reason for this may be expensive and continued experimental studies.

In [7, 8], such an approach was applied, where the influence of passing rolling stock on deformations in the spans of railroad bridges was revealed, the stress-strain state and dynamic coefficients of girder bridges were determined. However, there are issues related to the protection of strain gauges glued on the span structures for long-term monitoring of the technical condition of the spans. The reason for this may be objective difficulties related to the quality of adhesive and mastic tapes used to protect load cells from climatic and atmospheric precipitation. There is a high probability of "failures" – non-operability of strain gauges.

In [9], issues related to the use of AI in monitoring the condition of structures to maintain and secure infrastructure have been addressed. However, there is a high probability of failures in the signal transmission from the sensors to the receiver. Autonomy of this system, is questioned in prolonged power outage in case of terrorist attacks. A complete rejection of human participation in the processes of analyzing and making decisions on security issues is not reasonable.

The paper [10] presents the results and options of bridge condition monitoring (SHM) and their impact on the development of cyber-physical systems. But the issues related to the possibility of using this system on cable-stayed suspension structures are quite problematic, which makes the corresponding research incomplete. An option to overcome the relevant difficulties may be the financial component and the small number of such structures in a given region. that the development of intelligent technologies in SHM is based on innovative diagnostics in civil engineering. However, it is shown in [11] that the development of smart technologies in SHM is based on innovation diagnosis in civil engineering is very successful.

The paper [12] presents the results of the study of the interface of the approach embankment with the bridge and overpass. It is shown that there are objective difficulties associated with the installation of sensors in the embankment body and selection of appropriate equipment. The reasons for this may be (poor condition of tested structures, resolution of the protective layer of concrete, soaking of the structure, impossibility of approach under the bridge channel, etc.).

In [13], the results of damage investigation for seismically isolated bridges are presented. It is shown that the procedure of defect identification was used, but the localization of damage locations for metal bridges is not sufficiently covered.

In [14], research results and application of a technical code for monitoring buildings and bridge structures in China are presented. This study is not applicable to all bridge structures. The study of steel ropes and places of their fastening to span and suspension structures is not considered.

The papers [15–17] review the analysis and evaluation of the load-bearing capacity of existing railroad bridges with a deck made of poured girders. It is shown that the state of use of poured girder bridges in standard construction practice, significantly differs from similar studies of short-span poured girder bridges with rigid steel girders. However, the issues of aerodynamics and vibration at long spans remain unaddressed.

In [18], a bidirectional short-term memory method for infrastructure condition monitoring using on-board vibration was demonstrated. However, there is no clear understanding about the database, its accumulation storage location of the acquired data and subsequent processing.

In [19], an approach of digital twinning of self-sensing structures using statistical finite element method has been used. But the issues related to the determination of internal stress in elements with anisotropic medium are very doubtful, there is always a possibility of not taking into account one or another factor.

In [20], it is shown how to detect damage to a box girder of a high-speed railroad using dynamic responses caused by train motion. However, high-sensitivity equipment is usually very sensitive to electromagnetic fields, especially on long and massive metal objects on electrified railroad sections. The solution to this problem can be shielding of wires that transmit data from the sensor to the transducer, or mathematical filters to remove the 50 Hz component of interference in the signal.

In [21], a study of long-term monitoring of the condition of rail shoulders in turnstiles using extreme value distributions was carried out. However, there is a high probability of sensor failure due to their long-term stay in unfavorable natural and climatic conditions, which will certainly affect the research result.

In [22], the application of fiber optic sensors for structural monitoring of railway bridges is shown. However, there is a possibility of equipment failure due to incompatibility with some sensors operating on the analog system.

In [23], monitoring of the structural condition of a steel truss railroad bridge by studying its low frequency response was shown, exactly this approach was used in [24], monitoring the condition of a corroding steel truss bridge is given as an example. However, in these studies, there are still issues not disclosed on the study of seismic and anthropogenic nature of vibrations.

The analysis of the above sources reveals objective difficulties related to the complexity of the interaction processes between moving loads (i.e., rolling stock) and structure reactions (many different factors, elements, materials – from bridge structure, track and bracing), as well as the problem of obtaining representative experimental data for a wide range of bridge spans.

Works [1–8] present the results of research on real-time monitoring of artificial structures of railway infrastructure of Republic of Kazakhstan, in particular, focused on stress-strain behavior of bridge spans under operational loads. It is shown that the use of advanced information technologies significantly increases the efficiency of maintenance of these structures, facilitating the transition from scheduled repairs to state-of-the-art repairs. However, there are still unresolved issues related to the accuracy of predicting the mechanical characteristics of bridge spans under operational loads. All of this suggests the need for further research to refine these methods and adapt them to the unique features of the region's railroad infrastructure. This will not only improve the applicability of these technologies, but will also improve the safety, reliability and economic efficiency of the infrastructure in the long term.

To summarize, it can be noted that in order to detect hidden defects in bridge structures, it is necessary to monitor the technical condition of the entire artificial structure. Monitoring and various systems allowing to track and detect damage and hidden threats to the safe operation of railway infrastructure are of special importance. However, there are certain difficulties with selection of appropriate sensors and sensitivity of equipment, correctness of sensor installation, mathematical processing of received signals (selection of appropriate filters), data collection and storage, data analysis, etc.

3. The aim and objectives of the study

The aim of the study is to identify the stress-strain state of reinforced concrete girder spans based on monitoring data. This will allow to safely operate railway artificial structures and to pass on them heavier trains (up to 25 tons per axle).

To achieve this aim, the following objectives are accomplished:

– to analyze the obtained data of stress-strain state of reinforced concrete spans of two railway overpasses according to the results of field monitoring;

– to analyze the data of deflections, deformations and stresses measurements obtained under static loading;

– to analyze the obtained data and compare them with the normative values;

– to analyze the results obtained during dynamic testing of overpass spans.

4. Materials and methods

The object of the study was the girder spans of reinforced concrete railroad overpasses: 16.5 m – ribbed double-block T-shaped and 11.5 m – slab double-block T-shaped, roadway type – on crushed stone ballast. The tests were conducted in April 2018 and May 2023.

The main hypothesis of the research is the possibility detect hidden defects (threats) by investigating the stress-strain state of spanning structures using strain gauge method. The method of full-scale testing of bridge spans using a hardware and software system that realizes the interpretation and processing of digital records of primary transducers based on strainmetric means was used in the work. The monitoring system «TENZO» is used to determine the stress-strain state of span girders, which allows to detect internal forces in the structure, which makes it possible to analyze the obtained results and localize the defect locations. It is possible to select strain gauges for concrete of class B45, FLM-60-11 with an enlarged base of 60 mm, supplier: Japanese Measuring Technologies Ltd.

Fig. 1 shows the location of strain gauges on the spans of reinforced concrete railroad overpasses.

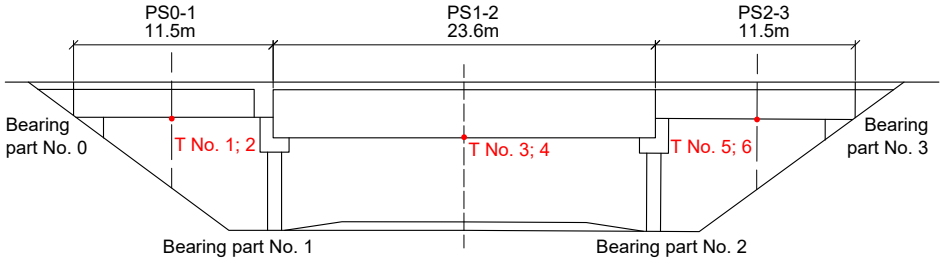

Fig. 1. Layout of strain gauges on reinforced concrete span structures of railway overpasses: overpass according to the scheme 11.5+23.6+11.5, PS0-1, PS1-2, PS2-3 – overpass span structures; T No. 1, T No. 2 T No. 3, T No. 4, T No. 5, T No. 6 – FLM-60-11 strain gauges; O No. 0, O No. 1, O No. 2, O No. 3 – backfill abutments and intermediate supports

Put away 16.5 + 23.6 + 16.5 m scheme.

Two intermediate supports No. 1 and No. 2 are equipped with massive reinforced concrete bollards to compensate for the difference in construction heights due to different span lengths, on which the outermost 16.5 m long spans are supported.

Spans of 16.5 m and design length of 15.8 m are reinforced concrete spans with ride on top under load C-14. Spans of 16.5 m full length and 15.8 m design length are ribbed two-block T-beams with two supporting diaphragms and twelve drainage pipes of 150 mm diameter.

The weight of one block is 53.2 tons. The rib width of one span block is 50 cm, the distance between the span blocks is 130 cm.

The span structure with the full length of 23.6 m and design length of 22.9 m is ribbed two-block, I-beam section with two supporting diaphragms and two intermediate diaphragms. The span girder consists of three longitudinal blocks. There are 16 drainage pipes of 150 mm diameter in the span. The weight of one span girder is 82.9 tons, all-transportable. The width of the girder rib at the bottom is 76 cm.

The 16.5 m spans are supported on tangential design supports designed for load C-14 (Fig. 2).

The number of support parts per one span is 4 pcs (two movable and two fixed). On supports No. 0 and No. 2 fixed and on supports No. 1 and No. 3 movable tangential support parts. The bearing parts consist of upper and lower balancers and a joint between them.

According to the standard design, the lower balancer is made with a tangential surface, the upper balancer with a horizontal flat surface.

The difference between the fixed bearing part and the movable bearing part is the size of the oval groove in the upper balancer.

At supports *b* and *c*, the supports are not made according to the design (inverted).

The 23.6 m span is supported on sector supports under load C-14.

The sector supports consist of an upper balancer, a hinge, a lower balancer in the form of a sector, a steel plate and a tooth to prevent possible displacement of the sector. The base plate is fixed to the sub-floor by 32 mm diameter anchor bolts.

The number of supporting parts per span is 4 pieces: two movable (Fig. 3) and two fixed (Fig. 4). On the support a there are fixed and on the support b there are movable sector support parts.

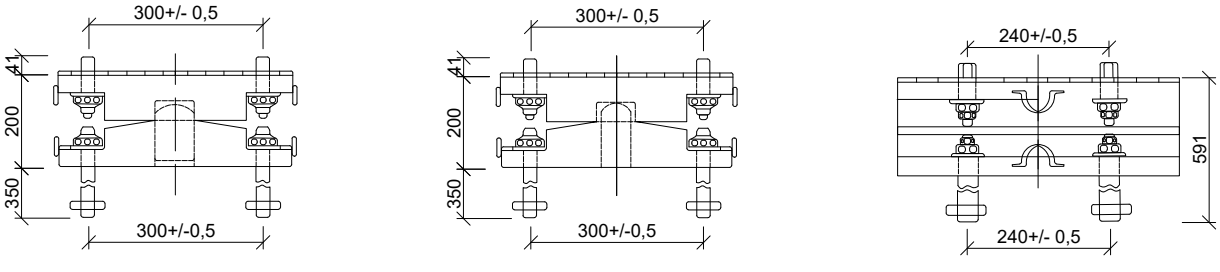

Fig. 2. Tangential support part: *a* – fixed part; *b* – support part; *c* – movable tangential support part

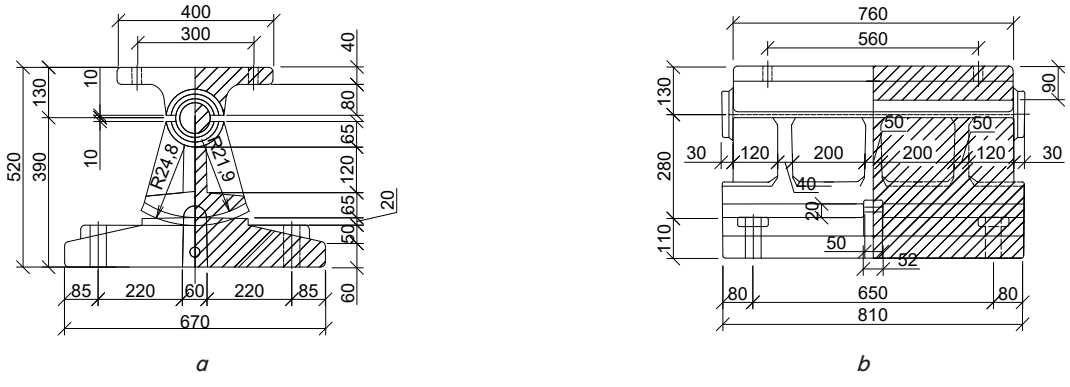

Fig. 3. Movable sector support part of PS: *a* – fixed par; *b* – support part

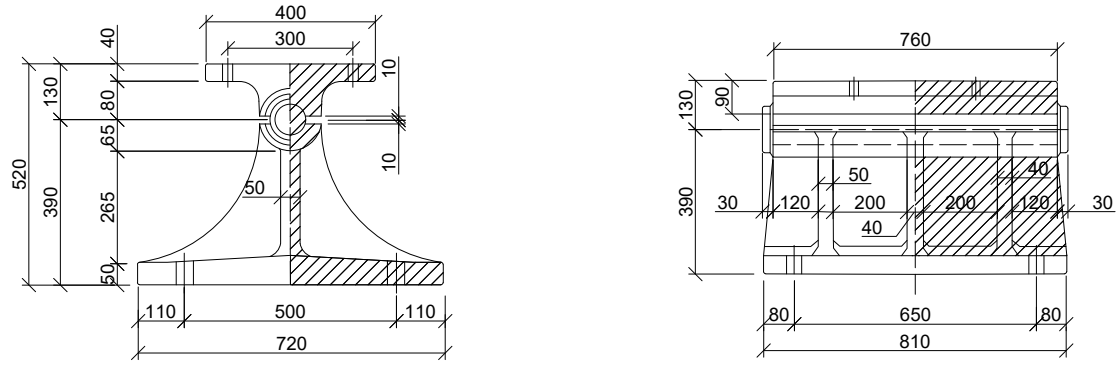

a *b*

Fig. 4. Fixed sector support part of PS: *a* — fixed part; *b* — support part

Puterway 11.5 + 23.6 + 11.5 m scheme.

Two intermediate supports *a* and *b* are equipped with massive reinforced concrete support bollards to compensate for the difference in construction heights due to different span lengths, on which the outermost 11.5 m long spans are supported, reinforced concrete with overhead ride under load C-14.

The full length of 11.5 m and the design length of 10.8 m spans are two-block plate spans with eight drainage pipes of 150 mm diameter.

The weight of one block is 37.5 tons. The width of a slab of one block of the span structure is 130 cm.

The average span of 23.6 m and design length of 22.9 m is prestressed with a ride on top under load C-14.

The full-length span of 23.6 m and design length of 22.9 m is ribbed double-block, I-beam section with two supporting diaphragms and two intermediate diaphragms. The span girder consists of three longitudinal blocks. There are 16 drainage pipes of 150 mm diameter in the span. The weight of one span girder is 82.9 tons, all-transportable. The width of the girder rib at the bottom is 76 cm.

Spans of 11.5 m are supported on tangential supports under load C-14.

The number of support parts per span is 8 pcs. The support parts consist of upper and lower balancers and a hinge between them (Fig. 2).

The 23.6 m span is supported on sector supports under load C-14.

The sector supports consist of an upper balancer, a hinge, a lower balancer in the form of a sector, a steel plate and a tooth to prevent possible displacement of the sector. The base plate is fixed to the sub-floor by 32 mm diameter anchor bolts.

The number of support parts per span is 4 pcs (two movable and two fixed) (Fig. 3).

On the support No. 1, there are movable and on the support No. 2 there are fixed sector support parts (Fig. 4).

Bridge bed at the two overpasses is analogous, with driving on crushed stone ballast, R-65 type rails, wooden sleepers, Pandrol fasteners, sleeper configuration 1840 pcs/km. The track is a link track, the rails are 25 m long, the rail joints are arranged on a try square. On the overpass the counter-rails of R-50 type rails with crutch fastening are laid. At a distance of 10 m from the rear faces of the foundations the counter rails are brought together by "shuttles", the ends of the rails are fastened with two bolts, the shoes are standard metal.

Separate side sidewalks are arranged at the spans on metal cantilevers attached to the sides of the spans from both sides.

The sidewalk decking is made of reinforced concrete slabs. The posts and handrails of the railing are made of 65 × 65 × 6 mm angles, the railing filling is made of two bars of reinforcement with a diameter of 20 mm.

The strain gauge-based software and hardware complex (SHC) is designed for measuring relative deformations and stresses in structures. This equipment enables: measurement of stresses and relative deformations in bridge span elements under the influence of rolling stock in 16 sections simultaneously, with a measurement track length of up to 500 meters (Fig. 5).

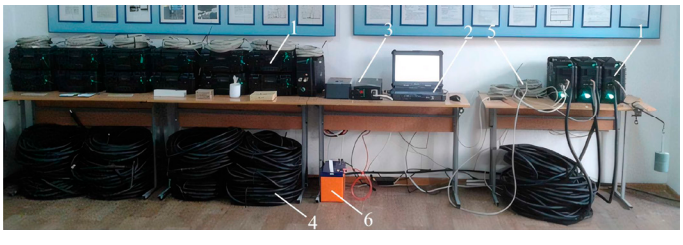

Fig. 5. Tensometric measuring and computing complex for measuring relative deformations and stresses in structures: 1 — measuring modules (16 pieces); 2 — semi-industrial laptop; 3 — sinusoidal inverter; 4 — intermodulation connection cable; 5 — connecting cable between the measuring module and the primary transducer (strain gage); 6 — accumulator battery

Configuration of the TMCC for testing artificial structure components, as shown in Fig. 6.

The TMCC (tensometric measuring and computing complex) consists of:

1. A rugged laptop with a high degree of casing protection (IP65), offering high performance and multiple input-output ports for data transfer [7, 8].

Due to its durable shockproof casing, resistance to vibrations and impacts, and support for solid-state drives, such laptops are often referred to as «military-grade».

2. Measuring electronics with an industrial bus "Module PME-55" (Fig. 7) operating mode capabilities are presented in Table 1, and technical characteristics in Table 2 [7, 8].

3. Strain gauges PFL-10-11 and FLM-60-11 (Fig. 8).

Strain gauges of the PFL and FLM series are designed for measuring the deformation of machine parts and structures or for use as sensing elements in measuring transducers. Manufacturer: Tokyo Sokki Kenkyujo Co., Ltd.

Supplier: LLC «Japanese Measurement Technologies» [7, 8].

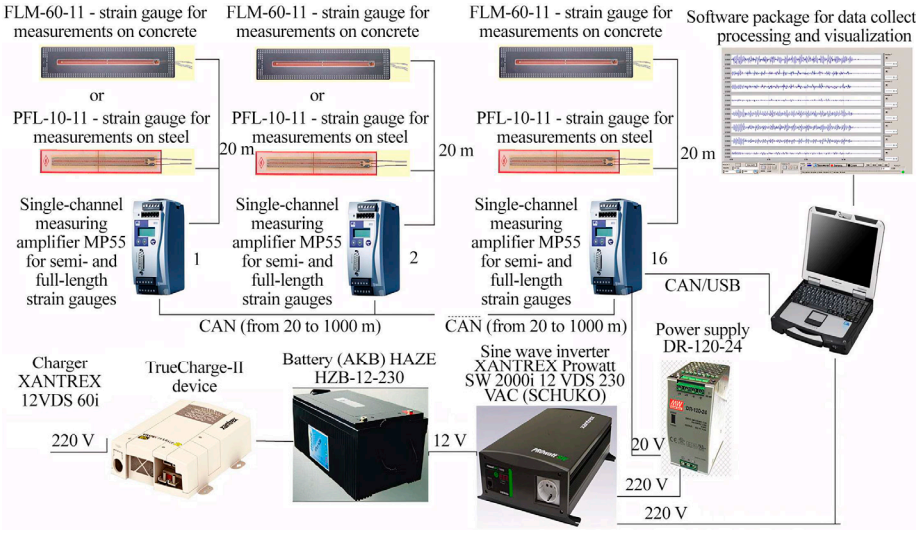

Fig. 6. Configuration of the tensometric measuring and computing complex for testing artificial structures

Fig. 7. Measuring electronics «Module PME-55»

Table 1

Operating mode capabilities of «Module PME-55»

No.	Sensor type and nominal characteristic	Bridge type	Bridge supply voltage	Input range
1	Strain gauge force sensor 2 mV/V = 20 kN	Full bridge	5 V	3 mV/V
2	Inductive displacement sensor 80 mV/V	Half bridge	2.5 V	100 mV/V
3	Inductive displacement sensor 10 mV/V	Half bridge	1 V	15 mV/V

The tensometric measuring and computing complex (TMCC) is designed for testing transport and construction structures. It measures various types of deformations in tested structures by recording and converting sensor signals into engineering units in real-time. The system presents the obtained data in the form of graphs and tables, storing it on a personal computer. The results have been published by the authors [7, 8]. Fig. 9–13 illustrate the application of TMCC and demonstrate typical measurement outputs obtained during experimental studies.

Static tests were carried out by employees of the research laboratory "Testing of track and artificial structures". The list of equipment is given in Tables 1, 2 the tests were carried out in accordance with the recommendations of SP RK 3.03-113-2014. Bridges and pipes.

During static tests the following parameters were measured deflections and relative deformations occurring in the middle of the lower part of the overpass span girders under the action of the test load.

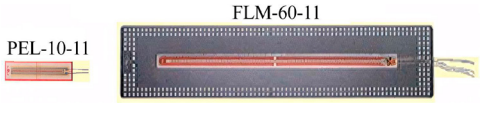

Fig. 8. Strain gauges for testing metal, concrete, and reinforced concrete structural elements

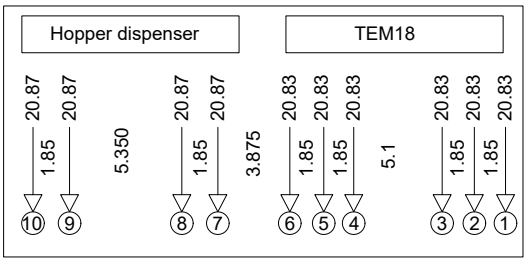

Fig. 9. Test load schemes in 2018 and 2023: Above – TEM18 diesel locomotive + hopper-dispenser model 55-76; Below – a train of 3 TEM18 diesel locomotives + 2 gondola cars

Table 2

Technical specifications of «Module PME-55»

Parameter	Unit	Value
Amplifier		
Carrier frequency	kHz	4.8 ± 1%
Dimensions ($W \times H \times D$)	mm	55 × 140 × 156
Weight (approx.)	g	750
Connected Sensors		
Half- and full-bridge strain gauges	Ohm	220…5000/110…5000/60…5000
Maximum allowable cable length between sensor and amplifier	m	max 500
Measured frequency range (–1 dB), adjustable	Hz	0.05…500
Interface		
Sampling rate (approx.)	–	max 1000 measured values/sec
Connection Bus		

Transmission speed	kbit/s	1000	500	250	125	100	50	20	10
Maximum cable length	m	25	100	250	500	600	1000	1000	1000

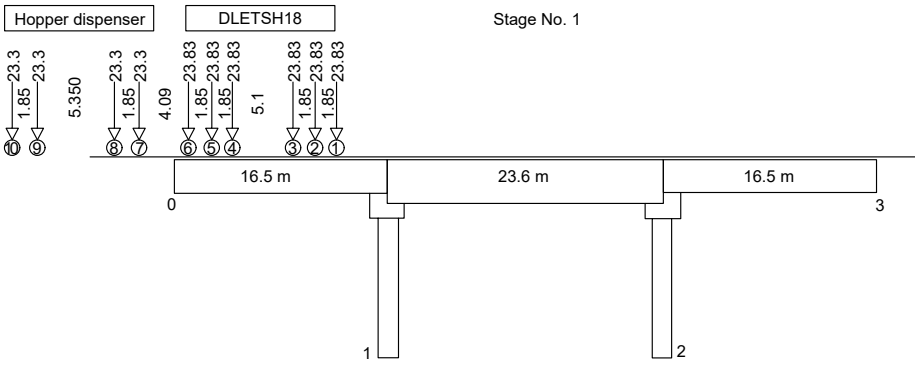

a

b

Fig. 10. Pipeline according to the scheme 16.5 + 23.6 + 16.5 in 2018: *a* – loading diagram for diesel locomotive TEM18 PS0-1 = 16.5 m; *b* – photo of test of superstructure PS0-1 = 16.5 m diesel locomotive TEM18

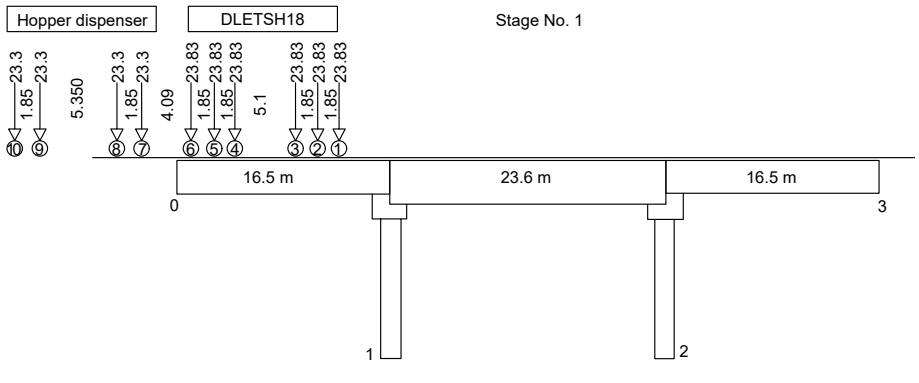

a

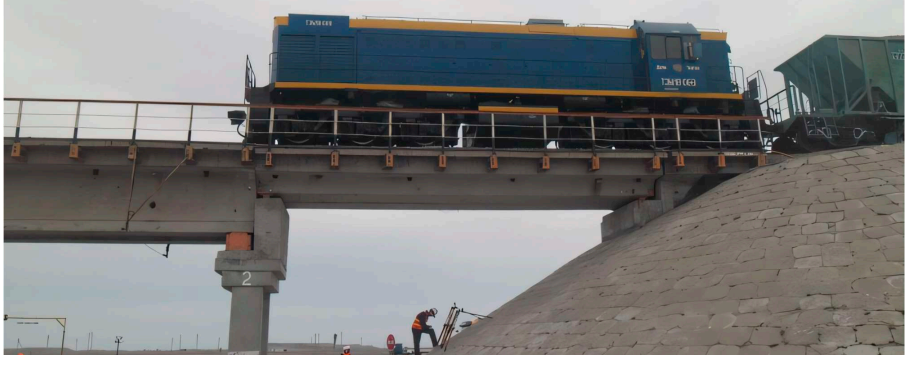

b

Fig. 11. Pipeline according to the scheme 11.5 + 23.6 + 11.5: *a* – loading diagram for diesel locomotive TEM18 PS0-1 = 11.5 m; *b* – photo of test of superstructure PS0-1 = 11.5 m diesel locomotive TEM18

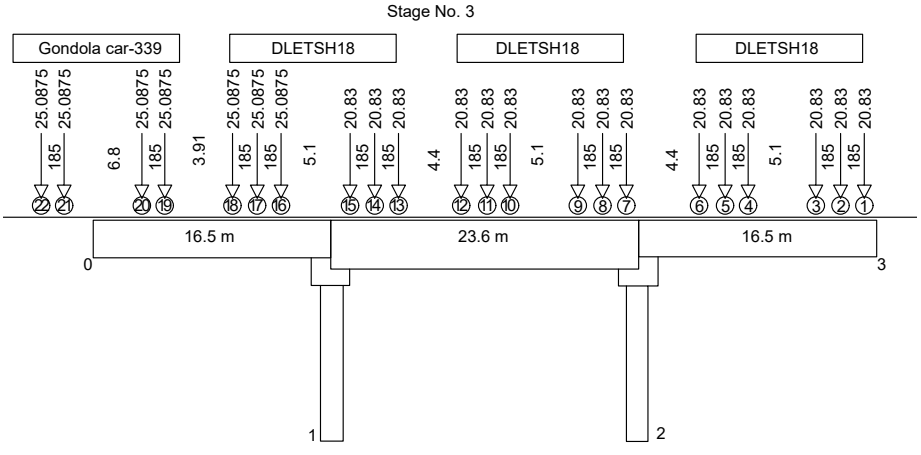

a

b

Fig. 12. Pipeline according to the scheme 16.5 + 23.6 + 16.5: *a* – loading diagram for diesel locomotive TEM18 PS0-1 = 16.5 m; *b* – photo of test of superstructure PS0-1 = 16.5 m diesel locomotive TEM18

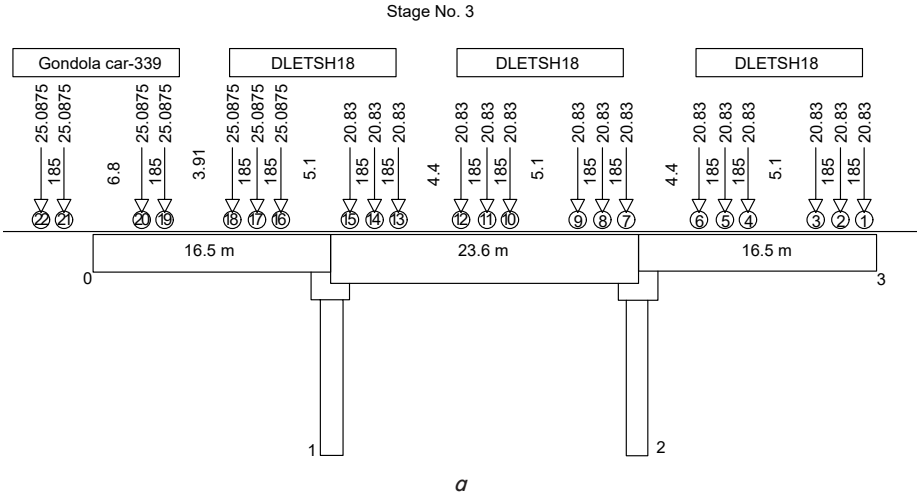

a

b

Fig. 13. Pipeline according to the scheme 11.5 + 23.6 + 11.5: *a* – loading diagram for diesel locomotive TEM18 PS0-1 = 11.5 m; *b* – photo of test of superstructure PS0-1 = 11.5 m diesel locomotive TEM18

The dynamic tests consisted of measurements of relative deformations (stresses) and deflections (displacements) occurring during the passage of the test load over the overpass at speeds of 10, 20, 30, 40 and 50 km/h. The values of dynamic coefficient (Tables 1, 2) were determined for the overpass spans under test load at different speeds [17, 18].

In 2018, the test load (Fig. 9, *a*) consisted of a 6-axle shunting diesel locomotive TEM-18 with an axle load of 20.7 tf (202.7 kN) and a 4-axle hopper-dosing car model 55–76 with an axle load of 23.3 tf (228.7 kN), and in 2023, the test load was a train (Fig. 10, *b*) consisting of 3 6-axle TEM-18 diesel locomotives with an axle load of 20.83 tf (204.3 kN) and 2 gondola cars with an axle load of 24.5625 tf (240.95 kN) – the first and 25.0875 tf (246.1 kN) the second [19].

5. Analysis of stress-strain behavior in reinforced concrete railway overpasses based on field monitoring and static load testing

5. 1. Field monitoring of stress-strain state of reinforced concrete span structures of two railway overpasses

The results of field monitoring of the stress-strain state of reinforced concrete span structures of two railway overpasses under operational loading conditions in 2018 and 2023 are presented. The measurements of displacements, relative deformations, and stresses were carried out on the superstructures of railway overpasses PS 0-1 and PS 2-3. The data obtained in 2018 and 2023 are shown in Tables 3–6.

Table 3

Measured displacements 16.5 + 23.6 + 16.5, relative deformations and stresses in overpass spans in 2018

No. of stage	Pipeline according to the scheme 16.5 + 23.6 + 16.5											
	PS 0-1						PS 2-3					
	Right block			Left block			Right block			Left block		
	mm	micrometer	MPa	mm	micrometer	MPa	mm	micrometer	MPa	mm	micrometer	MPa
1	4.30	120	3.71	4.23	126	3.90	0	0	0	0	0	0
5	0	0	0	0	0	0	4.12	119	3.70	3.77	112	3.46

Table 4

Measured displacements 11.5 + 23.6 + 11.5, relative deformations and stresses in overpass spans in 2018

No. of stage	Pipeline according to the scheme 11.5 + 23.6 + 11.5											
	PS 0-1						PS 2-3					
	Right block			Left block			Right block			Left block		
	mm	micrometer	MPa	mm	micrometer	MPa	mm	micrometer	MPa	mm	micrometer	MPa
1	2.75	110	3.78	2.63	103	3.55	0	0	0	0	0	0
5	0	0	0	0	0	0	2.84	101	3.46	2.66	99	3.41

Table 5

Measured displacements 16.5 + 23.6 + 16.5, relative deformations and stresses in overpass spans in 2023

No. of stage	Pipeline according to the scheme 16.5 + 23.6 + 16.5											
	PS 0-1						PS 2-3					
	Right block			Left block			Right block			Left block		
	mm	micrometer	MPa	mm	micrometer	MPa	mm	micrometer	MPa	mm	micrometer	MPa
1	4.33	133	4.11	4.34	135	4.16	0	0	0	0	0	0
2	4.71	168	5.40	4.77	165	5.08	0	0	0	0	0	0
3	0	0	0	0	0	0	3.95	123	3.82	3.40	112	3.48
5	0	0	0	0	0	0	4.15	137	4.25	3.65	122	3.76

Table 6

Measured displacements 11.5 + 23.6 + 11.5, relative deformations and stresses in overpass spans in 2023

No. of stage	Pipeline according to the scheme 11.5 + 23.6 + 11.5											
	PS 0-1						PS 2-3					
	Right block			Left block			Right block			Left block		
	mm	micrometer	MPa	mm	micrometer	MPa	mm	micrometer	MPa	mm	micrometer	MPa
1	0	0	0	0	0	0	2.37	75	2.58	2.35	78	2.67
3	0	0	0	0	0	0	2.52	85	2.92	2.54	83	2.83
3	2.55	82	2.82	2.63	84	2.88	0	0	0	0	0	0
4	3.72	125	4.29	3.53	128	4.39	0	0	0	0	0	0
5	3.49	134	4.58	3.42	137	4.70	0	0	0	0	0	0
6	3.49	135	4.65	3.45	130	4.48	0	0	0	0	0	0

The data presented in Tables 3–6 indicate a consistent pattern of stress-strain behavior under operational conditions across both monitoring periods. While some variations are observed between 2018 and 2023, they remain within the expected range for reinforced concrete structures of this type. These results suggest that the structural integrity of the overpasses has been maintained, with no significant deviations that would indicate progressive degradation.

5. 2. Measurements of deflections, deformations, and stress responses under static loading

Deflections, deformations, and stress responses resulting from static loading were measured using the «TENZO» hardware and software system, based on strain gauge sensors. The measurements were taken on reinforced concrete superstructures to evaluate the behavior under static loads. The stress diagrams of the reinforced concrete spans, 16.5 meters long, for spans PS 0-1 and PS 2-3, are shown in Fig. 14.

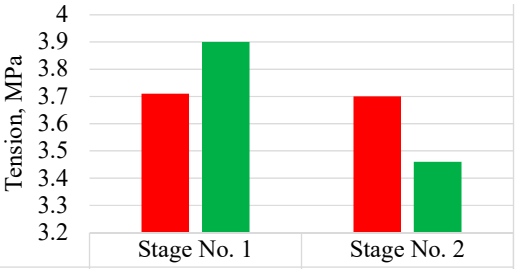

	Stage No. 1	Stage No. 2
Right block	3.71	3.7
Left block	3.9	3.46

a

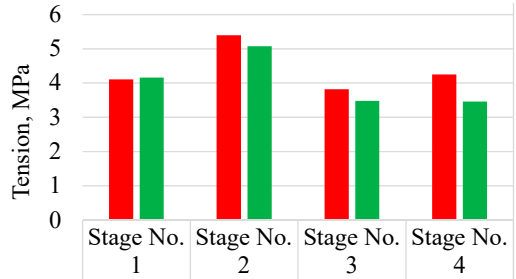

	Stage No. 1	Stage No. 2	Stage No. 3	Stage No. 4
Right block	4.11	5.4	3.82	4.25
Left block	4.16	5.08	3.48	3.46

b

Fig. 14. Span stress diagrams = 16.5 m of buildings in 2018 and 2023: a – PS 0-1 and PS 2-3 with a length of 16.5 m in 2018 from loading No. 1 and No. 5; *b* – PS 0-1 and PS 2-3 with a length of 16.5 m in 2023 from loading No. 1, No. 2, No. 3 and No. 5

Fig. 15 shows the stress diagrams of reinforced concrete spans 11.5 m long PS 0-1 and PS 2-3: on the left are the data obtained in 2018, on the right are the data obtained in 2023.

The stress distribution patterns shown in Fig. 14 reflect a stable structural performance under applied static loads. The obtained results demonstrate that the recorded stress levels do not exceed the design limits, confirming the adequacy of the structural system and the effectiveness of reinforcement. Minor discrepancies between individual measurements are attributed to local material heterogeneities and boundary conditions, but overall, the spans exhibit uniform load-bearing behavior with no critical stress concentrations.

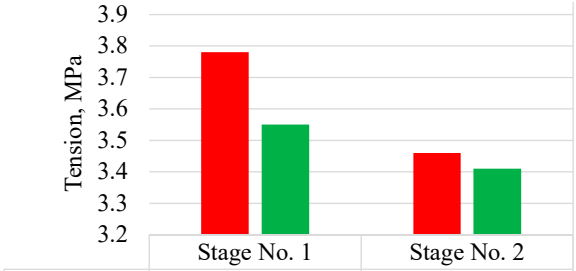

	Stage No. 1	Stage No. 2
Right block	3.78	3.46
Left block	3.55	3.41

a

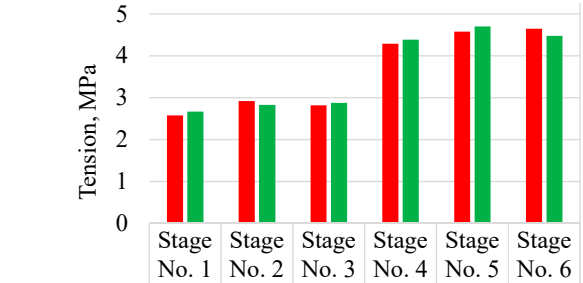

	Stage No. 1	Stage No. 2	Stage No. 3	Stage No. 4	Stage No. 5	Stage No. 6
Right block	2.58	2.92	2.82	4.29	4.58	4.65
Left block	2.67	2.83	2.88	4.39	4.7	4.48

b

Fig. 15. Span stress diagrams = 11.5 m of buildings in 2018 and 2023: a – PS 0-1 and PS 2-3 with a length of 16.5 m in 2018 from loading No. 1 and No. 5; *b* – PS 0-1 and PS 2-3 with a length of 16.5 m in 2023 from loading No. 1–No. 6

5. 3. Data analysis and comparison with normative values

Analyzing Fig. 14, 15, the following conclusions can be drawn.

In 2018, the "spread" of stresses from the test load (TEM18) for the right blocks of the 11.5 m spans was in the range of 3.7 MPa to 3.71 MPa at different loading stages, while for the left blocks of the 11.5 m spans, it ranged from 3.46 MPa to 3.9 MPa at different loading stages. In 2023, for the right blocks of the 11.5 m spans, the stress range was from 2.58 MPa to 4.65 MPa, and for the left blocks, it ranged from 2.67 MPa to 4.7 MPa at different loading stages [19, 20].

The 2018 data indicates uneven loading of the span blocks, which suggests a shift in the track axis away from the axis of the transport structure. For example, the difference in stress in the blocks for 11.5 m PS 0-1 at stage No. 1 was 5.12%, and at stage No. 5, it was 6.48%. For 16.5 m PS 0-1, the stress difference at stage No. 1 was 6.09%, and at stage No. 5, it was 1.44%.

In 2023, the span blocks worked uniformly, indicating that the track axis and the axis of the transport structure are aligned (coincide).

Tables 7–10 summarize the results of the deflections (displacements) of the overpass girder spans in 2018 and 2023.

The comparison of stress distribution and deflection values between the two monitoring periods highlights an improvement in structural behavior, most likely due to maintenance or track realignment. The observed data remain within normative limits, indicating no critical deformation or overloading. The enhanced uniformity of stress distribution in 2023 points to improved interaction between the superstructure and the applied loads, thus confirming the reliability of the span elements under operational conditions.

Table 7

Measured deflections (displacements) of the 16.5 + 23.6 + 16.5 m overpass in 2023

No. n/a	No. stage	PS 0-1		PS 1-2		PS 2-3	
		Right block	Left block	Right block	Left block	Right block	Left block
1	0	0	0	0	0	0	0
2-C1	1	4.33	4.34	0	0	0	0
3-C2	2	4.71	4.77	4.90	4.11	0	0
4-C3	3	4.76	4.99	4.73	4.20	3.95	3.40
5-C4	4	3.93	4.12	4.83	4.23	4.36	4.05
6-C5	5	0.21	0.23	4.80	4.23	4.15	3.65
7-C6	6	0	0	0	0	4.20	3.55
8	7	0	0	0	0	0	0

Note: 1 and 8 n/a (stages 0 and 7) – no loading.

Table 8

Measured deflections (displacements) of the 16.5 + 23.6 + 16.5 m overpass in 2018

No. n/a	No. stage	PS 0-1		PS 1-2		PS 2-3	
		Right block	Left block	Right block	Left block	Right block	Left block
1	0	0	0	0	0	0	0
2-C1	1	4.30	4.23	0	0	0	0
3-C2	2	4.49	4.56	2.90	2.41	0	0
4-C3	3	1.77	1.80	4.98	4.86	0	0
5-C4	4	0	0	4.98	4.98	0.64	0.60
6-C5	5	0	0	2.40	2.52	4.12	3.77
7-C6	6	0	0	0	0	4.33	4.03
8	7	0	0	0	0	0	0

Note: 1 and 8 n/a (stages 0 and 7) – no loading.

Table 9

Measured deflections (displacements) of the 11.5 + 23.6 + 11.5m overpass in 2023

No. n/a	No. stage	PS 0-1		PS 1-2		PS 2-3	
		Right block	Left block	Right block	Left block	Right block	Left block
1	0	0	0	0	0	0	0
2-C1	1	0	0	0	0	2.37	2.35
3-C2	2	0	0	4.70	4.77	3.54	3.48
4-C3	3	2.55	2.63	4.50	4.72	2.52	2.54
5-C4	4	3.72	3.53	4.70	4.82	3.74	3.68
6-C5	5	3.49	3.42	4.73	4.92	4.11	3.92
7-C6	6	3.49	3.45	4.19	4.32	0.30	0.30
8-C7	7	3.92	3.60	4.25	4.42	0	0
9-C8	8	4.05	3.82	1.28	1.30	0	0
10	9	0	0	0	0	0	0

Note: 1 and 10 n/a (stages 0 and 9) – no loading.

Table 10

Measured deflections (displacements) of the 11.5 + 23.6 + 11.5 m overpass in 2018

No. n/a	No. stage	PS 0-1		PS 1-2		PS 2-3	
		Right block	Left block	Right block	Left block	Right block	Left block
1	0	0	0	0	0	0	0
2-C1	1	0	0	0	0	2.75	2.63
3-C2	2	0	0	3.82	3.83	2.78	2.76
4-C3	3	0	0	4.90	4.99	1.85	1.78
5-C4	4	0.87	0.87	4.84	4.97	0	0
6-C5	5	2.84	2.66	3.94	3.99	0	0
7-C6	6	3.81	3.64	1.31	1.35	0	0
8-C7	7	2.86	2.70	0	0	0	0
9	8	0	0	0	0	0	0

Note: 1 and 9 n/a (stages 0 and 8) – no loading.

5. 4. Results of dynamic tests of overpass spans

The dynamic tests involved measuring the relative deformations (stresses) occurring when the test load passed over the overpass at speeds of 10, 20, 30, 40, and 50 km/h. The values of dynamic coefficients were determined for the overpass spans under different speed conditions.

Puterway 16.5 + 23.6 + 16.5 m scheme: the dynamic tests were carried out in 2018 and 2023, with the dynamic coefficients summarized in Tables 11–14. These tables show the impact of test load rates on the overpass spans under various speed conditions. Note: LB – Left Block; RB – Right Block [21, 22].

Puterway 11.5 + 23.6 + 11.5 m scheme: the dynamic tests in 2018 and 2023 for this scheme measured relative deformations (stresses) for different test load rates. The results are summarized in Tables 13, 14, with dynamic coefficients for each speed condition. Note: LB – Left block; RB – Right block [23, 24].

Table 11

Dynamic coefficient values in 2018

Speed, km/h	Dynamic coefficient, 1+μ					
	PS 0-1		PS 1-2		PS 2-3	
	LB	RB	LB	RB	LB	RB
10	1.13	1.11	1.07	1.12	1.12	1.10
20	1.17	1.15	1.07	1.12	1.16	1.14
30	1.14	1.15	1.11	1.01	1.13	1.14
40	1.21	1.18	1.11	1.12	1.20	1.17
50	1.16	1.19	1.11	1.12	1.15	1.18

Table 12

Dynamic coefficient values in 2023

Speed, km/h	Dynamic coefficient, 1+μ					
	PS 0-1		PS 1-2		PS 2-3	
	LB	PB	LB	PB	LB	PB
10	1.15	1.14	1.04	1.04	1.14	1.13
20	1.15	1.12	1.04	1.00	1.14	1.11
30	1.16	1.18	1.04	1.00	1.15	1.17
40	1.19	1.15	1.07	1.06	1.18	1.14
50	1.18	1.22	1.14	1.03	1.17	1.2

Table 13

Dynamic coefficient values in 2018

Speed, km/h	Dynamic coefficient, 1+μ					
	PS 0-1		PS 1-2		PS 2-3	
	LB	PB	LB	PB	LB	PB
10	1.04	1.01	1.00	1.07	1.12	1.03
20	1.00	1.02	1.00	1.11	1.16	1.04
30	1.05	1.02	1.04	1.07	1.13	1.04
40	1.08	1.06	1.07	1.18	1.20	1.08
50	1.08	1.14	1.12	1.18	1.15	1.16

Table 14

Dynamic coefficient values in 2023

Speed, km/h	Dynamic coefficient, 1+μ					
	PS 0-1		PS 1-2		PS 2-3	
	LB	PB	LB	PB	LB	PB
10	1.02	1.04	1.03	1.00	1.15	1.06
20	1.02	1.05	1.03	1.04	1.13	1.08
30	1.03	1.05	1.08	1.01	1.15	1.07
40	1.10	1.03	1.08	1.10	1.18	1.11
50	1.06	1.11	1.16	1.04	1.17	1.17

6. Discussion of the results of stress-strain state study by strain gauge method

Examining Tables 3–6, it is possible to see that the stress and strains of the structure behave consistently throughout both observation periods. Despite some changes, they remain within the permissible values for reinforced concrete structures. This indicates that the trestles retain their integrity and do not show signs of significant failure.

Analysis of Fig. 14, 15 allows conclusions to be drawn about the stresses in 2018 and 2023. The graphs indicate stable performance of the structure under static loads. The stress levels do not exceed the design values, which confirms the reliability of the structure and correct reinforcement. Small variations in the measurements can be attributed to variations in materials and operating conditions, but overall, the structures exhibit uniform behavior without dangerous stress concentrations. In 2018, the span blocks experienced non-uniform loads, indicating track axis displacement. In 2023, the blocks performed more uniformly, indicating alignment of the track axis and structure.

Tables 7–10 present the results of the span deflections for 2018 and 2023, the structure has performed better, likely due to maintenance or track changes. All values remain within normal limits, indicating that there are no major deformations.

In Tables 11–14, it is possible to see how the test load affects the structures at different speeds (10, 20, 30, 40 and 50 km/h). Dynamic coefficients were determined for the different span layouts in 2018 and 2023.

The strain gauge method allows diagnosing the presence of defects or internal damage to structures, unlike the visual method, which does not always detect internal defects.

The safety limitations of bridge structures are due to the fact that repair services do not allow opening the protective layer of concrete and load cells have to be glued directly onto the protective layer of concrete (fiber stress).

It is very important to properly glue the load cells to the structures, connect them to the main wires correctly and isolate them from natural and climatic influences (moisture, sun, etc.). To eliminate these disadvantages, the gluing places are specially prepared (ground with diamond disks, cleaned from dust, degreased), wires are soldered with dripping tin solder, and insulation is made with specially developed mastics (according to Japanese technologies) for monitoring systems.

The development of this research contributes to the improvement of systems for monitoring the technical condition of transportation objects. However, there are certain difficulties, as electromagnetic waves occur and wires need to be additionally shielded. Currently, researchers have the ability to make mathematical corrections for the electromagnetic component of 50 Hz interference.

The proposed method is based on the strain gauge method, by using fiber stresses and comparing them with the deflections of the spanning structures, the stress-strain state of the load-bearing elements is determined. With the help of this method it is possible to determine the current state and localize defects affecting the bearing capacity, reliability and stability of the whole structure.

Unlike the works [8, 9], which consider small-size automated systems for diagnostics and operation of artificial structures using information technologies, the proposed

method of diagnosing allows monitoring of spanning structures for several years, since strain gauges are protected by specialized materials of Japanese manufacture, similar to those of the authors [11–13].

Longitudinal monitoring of the stress-strain state of the spans over several years provides valuable information on the evolution of the behavior of the bridge elements and predicts possible degradation trends. This approach allows estimating the residual life and operational reliability of the structures under study.

The results obtained during the 2018 and 2023 monitoring campaigns support several important findings. First, the physical and mechanical condition of the girders of the surveyed railroad overpasses meets the requirements set out in the Rules of Technical Operation of Railroads of the Republic of Kazakhstan. This confirms that at the time of testing the structures remained serviceable and safe for further operation under the current loads. Secondly, the scatter of stress values in different elements of the span structure indicates the presence of possible structural abnormalities or hidden defects. These anomalies may be related to misalignment of the railroad track axis and the structural axis of the bridge or to uneven degradation of the material caused by environmental effects such as thermal cycling and moisture penetration.

The study confirms the effectiveness of advanced monitoring technologies, in particular the TENZO system, in providing detailed diagnostics of structural behavior. Such tools contribute to active maintenance planning, early detection of degradation and reduction of the cost of the railway infrastructure lifecycle. Adding real-time monitoring data to the asset management system also increases the security and stability of use.

While the study demonstrates the value of long-term monitoring, several limitations should be noted. The results are specific to the studied bridge structures and the environmental and operational conditions in which they were monitored. Therefore, their applicability to other structural types or regions with different climatic and loading conditions may be limited. The data represent behavior under specific test loads and controlled scenarios, which may not fully capture random dynamic effects or exceptional load cases. Additionally, the reproducibility of the results depends on the calibration accuracy and stability of the instrumentation used.

One key disadvantage is the limited number of span structures analyzed, which restricts the generalizability of the conclusions. The study also lacks a comparative analysis with other diagnostic methods, such as ultrasonic testing or material sampling, which could have strengthened the findings. In the future, extending the monitoring program to include a broader sample of structures, incorporating various load types (including extreme events), and integrating multidisciplinary diagnostic approaches would improve the robustness and applicability of the results.

7. Conclusions

1. In 2018, displacements, relative strains and stresses were measured in trestle spans 16.5 + 23.6 + 16.5. The maximum displacements for PS 0-1 were 4.3 mm (right block) and for PS 2-3 4. 12 mm (right block). The maximum relative strains for PS 0-1 were 126 μm (left block), for PS 2-3 119 μm (left block). The maximum recorded stresses for PS 0-1 were 3.71 MPa (right Block), for PS 2-3 3.70 MPa (right block).

At 2023, displacements, relative strains, and stresses were measured in the 16.5 + 23.6 + 16.5 trestle spans. The maximum displacements for PS 0-1 were 4.77 mm (left block) and for PS 2-3 4. 15 mm (right block). The maximum relative strains for PS 0-1 were 168 μm (Right block), for PS 2-3 137 μm (right block). The maximum recorded stresses for PS 0-1 were 5.40 MPa (right block), for PS 2-3 4.25 MPa (right block).

In 2018, displacements, relative strains and stresses were measured in the 11.5 + 23.6 + 11.5 trestle spans. The maximum displacements for PS 0-1 were 2.75 mm (right block) and for PS 2-3 were 2.84 mm (right block). The maximum relative strains for PS 0-1 were 110 μm (right block), for PS 2-3 101 μm (right block). The maximum recorded stresses for PS 0-1 were 3.78 MPa (right block), for PS 2-3 3.46 MPa (right block).

At 2023, displacements, relative strains, and stresses were measured in trestle spans 11.5 + 23.6 + 11.5. The maximum displacements for PS 0-1 were 3.72 mm (right block) and for PS 2-3 2.54 mm (left block). The maximum relative strains for PS 0-1 were 137 μm (left block). The maximum recorded stresses for PS 0-1 was 4.65 MPa (right block), for PS 2-3 2.92 MPa (right block).

2. Deflections, deformations and stress reactions occurring under static loading were measured using the TENZO software and hardware complex based on strain gauges. Measurements were performed on reinforced concrete spans to evaluate the behavior of the TEM-18 diesel locomotive under static loading. Stress diagrams of reinforced concrete spans of PS 0-1 and PS 2-3 with a length of 16.5 m show that in 2018, the left block is loaded 5% more than the right block (PS 0-1), the right block 7% more than the left block (PS 2-3). In 2023, when the length of PS 0-1 and PS 2-3 is 16.5 m, the right block is 6% more stressed than the left block (PS 0-1), the right block is 12% more stressed than the left block (PS 2-3). From the stress diagrams of reinforced concrete spans of PS 0-1 and PS 2-3 with a length of 11.5 m, it can be seen that in 2018, the right block is 6% more loaded than the left block (PS 0-1), the right block is 1.4% more loaded than the left block (PS 2-3). In 2023, when the length of PS 0-1 and PS 2-3 is 11.5 m, the right block is 3% more loaded than the left block (PS 0-1), the right block is 2.6% more loaded than the left block (PS 2-3).

3. According to the results obtained for 2018 and 2023, an analysis showing the “deformations and stresses” relationship for typical beam spans of 11.5 m and 16.5 m was performed, which allows to judge the technical condition of the structures of the investigated facilities to predict the assignment of repair works in order to maintain operational safety. The results of monitoring control slightly differ from the existing normative values to a lesser extent and from the previously accumulated data, which indicates the possibility of increasing the passage of more tonnage of transported cargo through these objects (increasing the axial load up to 25 tons per axle).

4. The dynamic test results show a consistent pattern across both structural schemes and testing years. The calculated dynamic coefficients remain within the normative thresholds defined by current engineering standards, indi-

cating stable dynamic performance under operational loading conditions. While minor variations between left and right blocks were observed, particularly at higher speeds, they do not suggest any critical imbalance or structural anomalies. Overall, the spans demonstrated reliable behavior under dynamic loads, with no evidence of significant degradation between 2018 and 2023.

Conflict of interest

The authors declare that they have no conflict of interest in relation to this study, whether financial, personal, authorship or otherwise, that could affect the study and its results presented in this paper.

Financing

The study was performed without financial support.

Data availability

Manuscript has no associated data.

Use of artificial intelligence

The authors of the article claim that they did not use artificial intelligence or other technologies. The article uses data obtained during experimental studies conducted by Ivan Bondar according to the methods approved by him [7, 8].

Acknowledgements

The author would like to express sincere gratitude to Satbayev University for their valuable support and contributions to this research. Their assistance in providing the necessary resources and expertise significantly enhanced the quality and scope of this study.

References

1. Abdullayev, S. S., Bondar, I. S., Bakyt, G. B., Ashirbayev, G. K., Budiukin, A. M., Baubekov, Ye. Ye. (2021). Interaction of frame structures with rolling stock. Series of Geology and Technical Sciences, 445 (1), 22–28. https://doi.org/10.32014/2021.2518-170x.3
2. Abdullayev, S. S., Bakyt, G. B., Aikumbekov, M. N., Bondar, I. S., Auyesbayev, Y. T. (2021). Determination of natural modes of railway overpasses. Journal of Applied Research and Technology, 19 (1), 1–10. https://doi.org/10.22201/icat.24486736e.2021.19.1.1487
3. Zhussupov, K., Toktamyssova, A., Abdullayev, S., Bakyt, G., Yessengaliyev, M. (2018). Investigation of the Stress-Strain State of a Wheel Flange of the Locomotive by the Method of Finite Element Modeling. Mechanics, 24 (2). https://doi.org/10.5755/j01.mech.24.2.17637
4. Abdullayev, S., Tokmurzina, N., Bakyt, G. (2016). The Determination of Admissible Speed of Locomotives on the Railway Tracks of the Republic of Kazakhstan. Transport Problems, 11 (1), 61–68. https://doi.org/10.20858/tp.2016.11.1.6
5. Zhumanov, A. U. (2018). Locomotive fleet of the Republic of Kazakhstan. Transport vehicles and equipment. Journal "Transport of the Russian Federation", 6 (79), 45–48.
6. Abdullayev, S., Imasheva, G., Tomkurzina, N., Adilova, N., Bakyt, G. (2018). Prospects for the Use of Gondola Cars on Bogies of Model ZK1 in the Organization of Heavy Freight Traffic in the Republic of Kazakhstan. Mechanics, 24 (1). https://doi.org/10.5755/j01.mech.24.1.17710
7. Bondar, I. S. (2016). Effect of moving load on deformations of the superstructure of a railway bridge. Collection of papers with international participation, 7, 64–67.
8. Bondar, I. S., Makhmetova, N. M., Kvashnin, M. Ya., Khasenov, S. S. (2023). Determination of the stress state and dynamic coefficients of beam bridges. Bulletin of the Siberian State Transport University, 4 (67), 92–100.
9. Plevris, V., Papazafeiropoulos, G. (2024). AI in Structural Health Monitoring for Infrastructure Maintenance and Safety. Infrastructures, 9 (12), 225. https://doi.org/10.3390/infrastructures9120225
10. Aktan, E., Bartoli, I., Glišić, B., Rainieri, C. (2024). Lessons from Bridge Structural Health Monitoring (SHM) and Their Implications for the Development of Cyber-Physical Systems. Infrastructures, 9 (2), 30. https://doi.org/10.3390/infrastructures9020030
11. Vijayan, D. S., Sivasuriyan, A., Devarajan, P., Krejsa, M., Chalecki, M., Żółtowski, M. et al. (2023). Development of Intelligent Technologies in SHM on the Innovative Diagnosis in Civil Engineering – A Comprehensive Review. Buildings, 13 (8), 1903. https://doi.org/10.3390/buildings13081903
12. Lanis, A., Razuvaev, D., Lomov, P. (2016). Conjugation of approach fill with bridge and overbridge. The Russian Automobile and Highway Industry Journal. 2 (48), 110–120.
13. Bonessio, N., Lomiento, G., Benzoni, G. (2011). Damage identification procedure for seismically isolated bridges. Structural Control and Health Monitoring, 19 (5), 565–578. https://doi.org/10.1002/stc.448
14. Yang, Y., Li, Q., Yan, B. (2017). Specifications and applications of the technical code for monitoring of building and bridge structures in China. Advances in Mechanical Engineering, 9 (1). https://doi.org/10.1177/1687814016684272
15. Vičan, J., Gocál, J., Odrobiňák, J., Hlinka, R. (2012). Analysis and Load-carrying Capacity Estimation of Existing Railway Filler-beam Deck Bridges. Sspjce, 7 (2), 5–14. https://doi.org/10.2478/v10299-012-0001-6
16. Kvočák, V., Kožlejová, V., Chupayeva, K. (2013). State of the Art in the Utilization of Deck Bridges with Encased Filler-Beams in the Standard Construction Practice. Sspjce, 8 (1), 107–114. https://doi.org/10.2478/sspjce-2013-0012

17. Odrobiňák, J., Bujňák, J., Žilka, J. (2012). Study on Short Span Deck Bridges with Encased Steel Beams. Procedia Engineering, 40, 333–338. https://doi.org/10.1016/j.proeng.2012.07.104
18. Samani, R. R., Nunez, A., De Schutter, B. (2024). A Bidirectional Long Short Term Memory Approach for Infrastructure Health Monitoring Using On-board Vibration Response. arXiv. https://doi.org/10.48550/arXiv.2412.02643
19. Febrianto, E., Butler, L., Girolami, M., Cirak, F. (2022). Digital twinning of self-sensing structures using the statistical finite element method. Data-Centric Engineering, 3. https://doi.org/10.1017/dce.2022.28
20. Wang, X., Zhuo, Y., Li, S. (2023). Damage Detection of High-Speed Railway Box Girder Using Train-Induced Dynamic Responses. Sustainability, 15 (11), 8552. https://doi.org/10.3390/su15118552
21. Barkhordari, P., Galeazzi, R., Blanke, M. (2021). Monitoring of Railpad Long-term Condition in Turnouts Using Extreme Value Distributions. arXiv. https://doi.org/10.48550/arXiv.2101.02567
22. Sasy Chan, Y. W., Wang, H.-P., Xiang, P. (2021). Optical Fiber Sensors for Monitoring Railway Infrastructures: A Review towards Smart Concept. Symmetry, 13 (12), 2251. https://doi.org/10.3390/sym13122251
23. Radicioni, L., Bernardini, L., Bono, F. M., Anghileri, M., Capacci, L., Cazzulani, G. et al. (2023). Structural Health Monitoring of a steel truss railway bridge studying its low frequency response. Ce/Papers, 6 (5), 876–885. https://doi.org/10.1002/cepa.2184
24. Saravanan, U., Lenka, K. (2023). On condition monitoring of a corroding steel truss bridge – a case study. Proceedings of the 14th International Workshop on Structural Health Monitoring. https://doi.org/10.12783/shm2023/36929